SIMULATION OF THE (p, T) PHASE DIAGRAM OF THE TEMPERATURE DRIVEN METAMAGNET α-FeRh

M.E. GRUNER* and P. ENTEL

Institute of Physics

University of Duisburg-Essen, Duisburg Campus, D-47048 Duisburg, Germany

(Received ...)

Abstract

We perform finite pressure Monte Carlo simulations of an effective spin-analogous model with coupled magnetic and lattice degrees of freedom, which has been previously proposed in order to explain the anomalous temperature driven metamagnetic phase transition in α-FeRh. The results are in reasonable agreement with the experimental (p, T) phase diagram. In particular the critical behavior of the system along the transition lines is analysed in detail.

Keywords: Metamagnetic transition, FeRh, magnetovolume effects, Monte Carlo simulations

1. INTRODUCTION

Metamagnetic behavior, i.e., the occurrence of a phase transition between two ordered magnetic phases, can be observed in many antiferromagnetic materials. Usually this is achieved by applying a magnetic field. In some cases, the materials also undergo a temperature driven metamagnetic transition. Such a behavior has been found by Fallot and Horcart (Fallot, 1938; Fallot and Horcart, 1939) for stoichiometrically ordered base centered cubic α-FeRh. Subsequent examinations showed that the lattice structure is not affected by the transition; only an isotropic expansion of the lattice constant of about 1% is observed (de Bergevin and Muldawer, 1961; Zakharov, Kadomtseva, Levitin and Ponyatovskii, 1964) upon heating. The low temperature phase has a collinear antiferromagnetic spin structure of type II with Fe moments of $3.3\,\mu_{\mathrm{B}}$ alternating in direction of one of the coordinate axes and vanishing

*Corresponding author. Tel.: +49-203-379-3564, Fax.: +49-203-379-3665, eMail: me@thp.Uni-Duisburg.DE

moments at the Rh sites (Shirane, Chen and Nathans, 1964; Kunitomi, Kohgi and Nakai, 1971). In the ferromagnetic phase, which is stable between $T_\mathrm{m} \approx 320\,\mathrm{K}$ and $T_\mathrm{C} = 670\,\mathrm{K}$ (Zakharov, Kadomtseva, Levitin and Ponyatovskii, 1964; Kouvel and Hartelius, 1962), the Fe moments remain with $3.2\,\mu_\mathrm{B}$ almost unchanged, while the Rh atoms carry in this case a moment of $0.9\,\mu_\mathrm{B}$ (Shirane, Chen, Flinn and Nathans, 1963). Application of hydrostatic pressure suppresses the ferromagnetic (FM) phase. Above a critical pressure of 6 GPa the system immediately transforms from the antiferromagnetic (AF) to the paramagnetic (PM) phase (Vinokurova, Vlasov and Pardavi-Horvath, 1976). The AF-FM phase transition is of first order whereas the FM-PM transition is continuous. The nature of the AF-PM transition has not been unanimously determined so far (Vinokurova, Vlasov and Pardavi-Horvath, 1976; Léger, Susse and Vodar, 1967; Veselago, Vinokurova, Vlasov, Kulikov *et al.*, 1988).

Technically, the occurrence of a temperature driven metamagnetic transition around room temperature might be exploited to develop high density recording media for future hard disks (Thiele, Maat and Fullerton, 2003). Due to the large entropy change $\Delta S(T_\mathrm{m}) \approx 15\,\mathrm{J\,kg^{-1}K^{-1}}$ at T_m (Zakharov, Kadomtseva, Levitin and Ponyatovskii, 1964; Kouvel, 1966; Ponomarev, 1972; Ricodeau and Melville, 1974; Annaorazov, Nikitin, Tyurin, Asatryan *et al.*, 1996) another possible application of FeRh would be the use as working material in so called magnetic refrigerators (Annaorazov, Asatryan, Myalikgulyev, Nikitin *et al.*, 1992; Annaorazov, Ünal, Nikitin, Tyurin *et al.*, 2002).

Although the occurrence of a temperature driven metamagnetic transition in FeRh is known for quite a long time, a satisfactory explanation has not been given for several decades. Most attempts failed to meet the experimental facts in one aspect or the other (for a review of the most successful explanations see Gruner, Hoffmann and Entel (2003); Gruner (2003)). Recently, another explanation has been given by Gruner *et al.* (Gruner, Hoffmann and Entel, 2003). The authors assume that Fe and Rh moments have a mainly localized character and that the magnetic properties are governed by competing interactions: A FM exchange between nearest neighbor Fe and Rh spins, and an AF exchange between the next nearest neighbor Fe atoms. The most important point is, that the Rh moments are close to an instability, i.e., they can occur in two different spin states, which lie close in energy: A nonmagnetic ground state and a magnetic state with a moment of about $1\ \mu_\mathrm{B}$. As shown by Gruner, Hoffmann and Entel (2003), these considerations are confirmed by the results of *ab initio* calculations. Also, the thermodynamical properties of the model at finite temperatures, obtained by means of Monte-Carlo simulations, agree well with the experimental data. It turns out that in the FM phase the excitation of nonmagnetic Rh spins is more likely than the excitation of Rh spins with a finite moment in the AF Phase. This leads to an excess entropy in the FM phase capable of changing the sign in the free energy difference between the two phases. Especially the size of the

entropy change at the metamagnetic transition and the energy difference at low temperatures are in close agreement with the experimental observations. Lately, *ab initio* investigations by Mryasov (2004) indicate that also higher order exchange terms may play an important role.

The calculations presented by Gruner, Hoffmann and Entel (2003) describe only the properties of the model at zero pressure. Therefore, the purpose of this work is to extend the investigation to finite pressures and the comparison of the results with the experimental (p, T) phase diagram.

2. TECHNICAL DETAILS

As discussed in detail in (Gruner, Hoffmann and Entel, 2003), the instability of the Rh-moment can be described by a spin-1 Ising Hamiltonian with competing ferromagnetic and antiferromagnetic interactions depending on the type of elements involved. The dependence of the exchange parameters on the interatomic distances leads to realistic magnetovolume effects. The Hamiltonian consists of the following terms:

$$H = -\sum_i D_i\, S_i^2 - \sum_{<\mathrm{nn,nnn}>} J_{ik}(r_{ik})\, S_i\, S_k + \sum_{<\mathrm{nn}>} V_{\mathrm{nn}}(r_{ik}) + \sum_{<\mathrm{nnn}>} V_{\mathrm{nnn}}(r_{ik})\,. \quad (1)$$

The first two terms represent the well known Blume-Capel Hamiltonian (Blume, 1966; Capel, 1966). The $V(r_{ik})$ are simple pair potentials of Lennard-Jones type:

$$V(r_{ik}) = 4\,\epsilon \left[\left(\frac{\sigma}{r_{ik}}\right)^{12} - \left(\frac{\sigma}{r_{ik}}\right)^{6} \right]\,. \quad (2)$$

Different pair potentials for nearest and next nearest neighbor interactions are needed in order to stabilize the bcc lattice structure. The parameters used in our simulations are listed in Tables 1 and 2.

The calculation of the (p, T) phase diagram of our model system necessitates the evaluation of the Hamiltonian (1) at various pressures and temperatures. For this purpose we used a standard textbook isothermal-isobaric Monte Carlo method, see, e.g. Allen and Tildesley (1987), which has also been used in our previous simulations (Gruner, Meyer and Entel, 1998; Gruner and Entel, 2002; Gruner, Hoffmann and Entel, 2003). We refer to these publications for a comprehensive description of the calculational details.

The system sizes considered in our investigation range from $L = 12$ and $L = 16$ for the thermodynamic integration up to $L = 32$ and $L = 48$ for the analysis of the critical behavior at the FM-PM transition line. Here, L denotes the linear extension of the simulation cell in units of the lattice constant.

In general, simulation lengths of 400.000 to 800.000 lattice sweeps per run proved to be sufficient for obtaining accurate results whereas the analysis of the nature of the FM-PM phase transition required up to 10.000.000 lattice

sweeps per temperature ($p = 0.5\,\mathrm{GPa}$). For these calculations the use of parallel computers was indispensable.

3. DETERMINATION OF THE PHASE DIAGRAM

3.1. The AF-FM Transition

The transition lines between the two ordered phases are determined by calculating the difference ΔG between the Gibbs free enthalpies of the two phases along a line of constant pressure:

$$\Delta G(T)|_{p=\mathrm{const}} \;=\; \Delta E(T) \;-\; T\left(\Delta S(0) \;+\; \int_0^T \frac{\Delta C_p}{T}\; dT\right) \;+\; p\,\Delta V\,. \qquad (3)$$

The transition temperatures T_m are given by the intersection of ΔG with the abscissa (cf Fig. 1). As described by Gruner, Hoffmann and Entel (2003), the entropy at zero temperature, $\Delta S(0)$, can be calculated using the second derivative of the binding enthalpy curve, $E(V)+pV$, taken at the equilibrium volume assuming that $\Delta S(0)$ can be approximated by the entropy of an ensemble of harmonic oscillators at zero temperature. The values of $\Delta S(0)$ obtained in this way at various pressures are listed in Table 3 together with other important quantities like the volume changes and entropy differences at T_m.

In order to test the accuracy of our calculations, additional integrations have been performed by using Monte Carlo data gathered along a line of constant temperature (see Fig. 2):

$$\Delta G|_{T=\mathrm{const}} = \Delta G(p_1) + \int_{p_1}^{p_2} (V_\mathrm{FM} - V_\mathrm{AF})\; dp\,. \qquad (4)$$

By comparing the different results we obtain a maximum error of $\Delta T_\mathrm{m} = \pm 7\,\mathrm{K}$ for the determination of the transition temperature T_m and $\Delta p_\mathrm{m} = \pm 0.06\,\mathrm{GPa}$ for the determination of the transition pressure p_m.

3.2. The FM-PM Transition

In order to understand the behavior of the model at the FM-PM transition line, one must keep in mind that the phase diagram of the original Blume Capel model is characterized by first and second order phase transitions in the (T, D)-plane, whereby the corresponding transition lines are separated by a tricritical point. Considering the extended Hamiltonian given by Eq. (1), the special case of applying external pressure will similarly reduce the effective exchange parameteres with respect to D. Therefore, it is plausible to assume thatfor a particular choice of parameters a multicritical point in the

(p, T)-phase diagram of Eq. (1) can be observed. Indeed, we find a discontiuous behavior of the magnetization at larger pressures $p \gtrsim 2\,\mathrm{GPa}$ connected with a considerable hysteresis, whereas at $p = 0$ the order parameter decays smoothly at T_C. The corresponding Curie temperatures at different pressures are listed in Table 4. In order to confirm the second order nature of the phase transion at $p = 0$, we analyzed the critical behavior of the system using finite size scaling. For the Blume Capel model Ising universality is expected along the line of second order transition. Assuming the Ising critical exponents also to be valid in our case, we made data collapse plots for different system sizes, which confirmed the Ising universality at T_C within the accuracy of our calculations (Fig. 3).

However, at a pressure of 0.5 GPa, this method does not lead to satisfactory results with the Ising exponents. Furthermore, we have not been able to identify another consistent set of critical exponents which would allow the data of different system sizes to collapse onto a single curve. Therefore, this is a hint to a first order phase transition in this case. This can be verified with the help of the probability distribution function of the enthalpy, $P(E + pV)$, which is expected to exhibit a bimodal distribution at a first order phase transition (Challa, Landau and Binder, 1986). In fact, we observe a shoulder in $P(E)$ for the largest system size considered, which is $L = 48$ (cf Fig. 4). Two clearly distinct peaks can be found at $p = 1.5\,\mathrm{GPa}$ already at the moderate system size $L = 16$.

3.3. The AF-PM Transition

The transition temperature of second order phase transitions are determined by means of the second order and fourth order cumulant method (Binder, 1981; Binder, Vollmayr, Deutsch, Reger *et al.*, 1992; Binder, 1997) which could be performed along the AF-PM transition line without any difficulties (Tab. 5). We found second order phase transitions throughout the examined pressure range and a finite size scaling analysis clearly showed Ising-like critical behavior (Gruner, 2003).

4. DISCUSSION

The data collected from the calculations, which were discussed in the previous section, lead to the phase diagram shown in Fig. 5, which agrees reasonably well with experiment. There are, however, some obvious differences. The three transition lines join in one point, which can be estimated to $T_\mathrm{tr} = 597\,\mathrm{K}$ and $p_\mathrm{tr} = 26.5\,\mathrm{GPa}$ while the experimental value of p_tr is about twice as large. Also, the dependence of the FM-PM transition temperature on pressure is much larger than in experiment. Both disagreements can be traced back to an *ad hoc* assumption made when choosing the parameters that presupposes a linear dependence between $\partial J_{ik}/\partial r$ and $\partial T_{\mathrm{C,N}}/\partial p$. This is true for the

case that the bulk modulus remains constant along the FM-PM and AF-PM transition lines. However, due to the large magnetovolume effects at the FM-PM phase transition, this assumption does not hold anymore, leading to a much steeper decrease and thus to a premature end of the FM-PM transition line. The occurence of first order FM-PM transitions, which is likewise not backed by experimental data, can also be related to this problem.

In summary, the simple spin analogous model presented by Gruner, Hoffmann and Entel (2003) has proven that it allows a reasonable description of the properties of α-FeRh at finite pressures. Improvements can be made by a more accurate choice of parameters that could be based on the calculations presented in this paper and by small extensions of the model. One possible extension consists in altering the statistical weight of the $S_i = 0$ state compared to the $S_i = \pm 1$ states, as already done for Fe-Ni systems (Gruner, Meyer and Entel, 1998). This is permissible, since the $S_i = 0$ and $S_i = \pm 1$ states are the effective representations of bandstructure effects. So far, we used the same weight for all three states, which is a natural choice for the spin-1 Ising model. For the real system, however, this is somewhat arbitrary, since we have no information about the electronic origin of the formation of magnetic moment on the Rh sites. A second and important extension consists of replacing the discrete Ising-like character of the spins by Heisenberg-like degrees of freedom. Refering to Mryasov (2004), also biquadratic exchange interactions should be taken into account. This is under present consideration.

Acknowledgements

M. E. Gruner would like to thank O. N. Mryasov for fruitful discussions concerning the FeRh problem.

References

Allen, M. P. and D. J. Tildesley (1987). *Computer Simulation of Liquids*. Clarendon, Oxford.

Annaorazov, M. P., K. A. Asatryan, G. Myalikgulyev, S. A. Nikitin *et al.* (1992). Alloys of the Fe-Rh system as a new class of working material for magnetic refrigerators. *Cryogenics* **32**, 867.

Annaorazov, M. P., S. A. Nikitin, A. L. Tyurin, K. A. Asatryan *et al.* (1996). Anomalously high entropy change in FeRh alloy. *J. Appl. Phys.* **79**, 1689.

Annaorazov, M. P., M. Ünal, S. A. Nikitin, A. L. Tyurin *et al.* (2002). Magnetocaloric heat-pump cycles based on the AF-F transition in Fe-Rh alloys. *J. Magn. Magn. Mater* **251**, 61.

Binder, K. (1981). Finite size scaling analysis of Ising block distribution functions. *Z. Phys. B* **43**, 119.

Binder, K. (1997). Applications of Monte Carlo methods to statistical physics. *Rep. Prog. Phys.* **60**, 487.

Binder, K., K. Vollmayr, H. P. Deutsch, J. D. Reger *et al.* (1992). Monte Carlo methods for first order phase transitions: Some recent progress. *Int. J. Mod. Phys. C* **3**, 1025.

Blume, M. (1966). Theory of the first-order magnetic phase change in UO_2. *Phys. Rev.* **141**, 517.

Capel, H. W. (1966). On the possibility of first-order phase transitions in Ising systems of triplet ions with zero-field splitting. *Physica* **32**, 966.

Challa, M. S. S., D. P. Landau and K. Binder (1986). Finite-size effects at temperature-driven first-order transitions. *Phys. Rev. B* **34**, 1841.

De Bergevin, F. and L. Muldawer (1961). Étude cristallographique de certains alliage fer-rhodium. *C. R. Acad. Sci.* **252**, 1347.

Fallot, M. (1938). Les alliages du fer avec les métaux de la famille du platine. *Ann. Phys. (Paris)* **10**, 291.

Fallot, M. and R. Horcart (1939). Sur l'apparition du ferromagnétisme par élévation de température dans des alliages de fer et de rhodium. *Rev. Scient.* **77**, 498.

Gruner, M. E. (2003). Monte-Carlo-Simulationen von Magnetovolumeneffekten in Festkörpern und Nanopartikeln. Thesis, University of Duisburg-Essen, http://purl.oclc.org/NET/duett-01062004-171249.

Gruner, M. E. and P. Entel (2002). High-moment – low-moment description of magnetovolume effects in $Y(Mn_xAl_{1-x})_2$ and $Y_xSc_{1-x}Al_2$. *Phase Transitions* **75**, 221.

Gruner, M. E., E. Hoffmann and P. Entel (2003). Instability of the rhodium magnetic moment as the origin of the metamagnetic phase transition in α-FeRh. *Phys. Rev. B* **67**, 064415.

Gruner, M. E., R. Meyer and P. Entel (1998). Monte Carlo simulations of high-moment – low-moment transitions in Invar alloys. *Eur. Phys. J. B* **2**, 107.

Kouvel, J. S. (1966). Unusual nature of the abrupt magnetic transition in FeRh and its pseudobinary variants. *J. Appl. Phys.* **37**, 1257.

Kouvel, J. S. and C. C. Hartelius (1962). Anomalous magnetic moments and transformations in the ordered alloy FeRh. *J. Appl. Phys. Suppl.* **33**, 1343.

Kunitomi, N., M. Kohgi and Y. Nakai (1971). Diffuse scattering of neutrons in the antiferromagnetic phase of FeRh. *Phys. Lett. A* **37A**, 333.

Le Guillou, J. C. and J. Zinn-Justin (1980). Critical exponents from field theory. *Phys. Rev. B* **21**, 3976.

Léger, J. M., C. Susse and M. Vodar (1967). Point triple dans les diagrammes des phases P-T de deux alliages à base de fer et de rhodium. *C. R. Acad. Sci.* C **265**, 892.

Mryasov, O. N. (2004). Magnetic Interactions and Phase Transformations in FeM, M = (Pt,Rh) Ordered Alloys. *Phase Transitions*, this issue.

Ponomarev, B. K. (1972). Investigation of the antiferro-ferromagnetism transition in an FeRh alloy in a pulsed magnetic field up to 300 kOe. *Zh. Eksp. Teor. Fiz.* **63**, 199 [Sov. Phys. JETP **36**, 105 (1973)].

Ricodeau, J. A. and D. Melville (1974). High field magnetostriction in a metamagnetic FeRh alloy. *J. Physique I* **35**, 149.

Shirane, G., C. W. Chen, P. A. Flinn and R. Nathans (1963). Hyperfine fields and magnetic moments in the Fe-Rh system. *J. Appl. Phys.* **34**, 1044.

Shirane, G., C. W. Chen and R. Nathans (1964). Magnetic moments and unpaired spin densities in the Fe-Rh alloys. *Phys. Rev.* **134**, A1547.

Thiele, J.-U., S. Maat and E. E. Fullerton (2003). FeRh/FePt exchange spring films for thermally assisted magnetic recording media. *Appl. Phys. Lett.* **82**, 2859.

Veselago, V. G., L. I. Vinokurova, A. V. Vlasov, N. I. Kulikov *et al.* (1988). Instability of magnetic states in ordered iron-platinum and iron-rhodium alloys. In V. G. Veselago and L. I. Vinokurova, editors, *The Magnetic and Electron Structures of Transition Metals and Alloys*, volume 3, 45–81. Proceedings of the Institute of General Physics of the Academy of Sciences of the USSR, Nova Science, Commack.

Vinokurova, L. I., A. V. Vlasov and M. Pardavi-Horvath (1976). Pressure effects on magnetic phase transitions in FeRh and FeRhIr alloys. *Phys. Stat. Sol. B* **78**, 353.

Zakharov, A. I., A. M. Kadomtseva, R. Z. Levitin and E. G. Ponyatovskii (1964). Magnetic and magnetoelastic properties of a metamagnetic iron-rhodium alloy. *Zh. Eksp. Teor. Fiz.* **46**, 2003 [Sov. Phys. JETP **19**, 1348 (1964)].

TABLE CAPTIONS

Table 1:
Magnetic parameters for the spin model described by Eq. (1). A linear dependence of the exchange parameters on the interatomic distance is assumed. The exchange between the Rh-sites is neglected. Energies are specified in mRy, distances in Å.

Table 2:
Elastic parameters for the Lennard-Jones pair potentials (energies in mRy, distances in Å).

Table 3:
Differences of the enthalpies and entropies between the AF- and FM-Phases at $T = 4\,\mathrm{K}$ and the entropy change $\Delta S(T_\mathrm{m})$ and relative volume change $\Delta V/V$ at the metamagnetic transition temperature T_m.

Table 4:
The Curie temperatures as obtained by the MC simulations at pressures between 0 GPa and 2 GPa and from the experimental phase diagram (Veselago, Vinokurova, Vlasov, Kulikov *et al.*, 1988).

Table 5:
The Néel temperatures as obtained by the MC simulations at pressures between 3 GPa and 10 GPa and from experiment (Veselago, Vinokurova, Vlasov, Kulikov *et al.*, 1988).

FIGURE CAPTIONS

Figure 1:
The differences of Gibbs' free enthalpies, ΔG, between the AF- and FM-Phases at various pressures as a function of temperature. The curves were obtained by thermodynamic integration of the MC data along a line of constant pressure (system size: $L = 16$). The cirles denote experimental values for ambient pressure (Ponomarev, 1972).

Figure 2:
The differences of Gibbs' free enthalpies, ΔG, obtained by a thermodynamic integration along the path of constant temperature (lines). The circles refer to the corresponding values obtained by integration along a line of constant pressure (cf. Fig. 1).

Figure 3:
Finite size scaling plots of the magnetization $\langle |M| \rangle$ (left), susceptibility χ_{FM} (center) and specific heat C_p (right) at $p = 0$. A data collapse can be achieved by assuming that the 3d-Ising critical exponents can be used: $\beta = 0.325$, $\gamma = 1.24$, $\alpha = 0.11$, $\nu = 0.63$ (Le Guillou and Zinn-Justin, 1980).

Figure 4:
Probability distribution function $P(E + pV)$ of the enthalpy for $p = 0.5\,\mathrm{GPa}$ in close vicinity to the FM-PM phase transition at $T = 702\,\mathrm{K}$. The linear system size is $L = 48$. The inset shows $P(E+pV)$ for $p = 1.5\,\mathrm{GPa}$ at $T = 654\,\mathrm{K}$ ($L = 48$).

Figure 5:
The (p, T) phase diagram of the spin analogous model system from Eq. (1) obtained with the parameters of Tables 1 and 2. The circles denote the results of the simulations, the lines are interpolations. First order phase transitions are marked by dashed lines, continuous phase transitions by solid lines. The inset shows the experimental phase diagram (Veselago, Vinokurova, Vlasov, Kulikov *et al.*, 1988).

D_{Fe}	D_{Rh}	$J^{\mathrm{nn}}_{\mathrm{FeRh}}(2.6\ \text{Å})$	$J^{\mathrm{nnn}}_{\mathrm{FeFe}}(3.0\ \text{Å})$	$\partial J^{\mathrm{nn}}_{\mathrm{FeRh}}/\partial r$	$\partial J^{\mathrm{nnn}}_{\mathrm{FeFe}}/\partial r$
$\gg k_{\mathrm{B}}\,T$	-11.1	2.10	-1.04	1.97	1.58

Table 1: M. E. Gruner *et al.*

ϵ_{nn}	σ_{nn}	ϵ_{nnn}	σ_{nnn}
25.23	2.32	25.23	2.67

Table 2: M. E. Gruner *et al.*

	$T = 4\,\mathrm{K}$		$T = T_{\mathrm{m}}$		
p (GPa)	$\Delta(E+pV)$ (mRy)	$\Delta S(0)$ ($\mathrm{J\,kg^{-1}K^{-1}}$)	T_{m} (K)	$\Delta S(T_{\mathrm{m}})$ ($\mathrm{J\,kg^{-1}K^{-1}}$)	$\Delta V/V$ (%)
0.0	0.2275	9.185	324	15.83	0.90
1.0	0.2782	8.785	386	14.42	0.86
2.0	0.3273	8.420	457	10.24	0.80
2.5	0.3511	8.249	503	6.47	0.74
3.0	0.3746	8.085			

Table 3: M. E. Gruner *et al.*

p (GPa)	0	0.5	1.0	1.5	2.0
$T_{\mathrm{C,sim}}$ (K)	728	702	677	654	631
$T_{\mathrm{C,exp}}$ (K)	670	663	656	650	643

Table 4: M. E. Gruner *et al.*

p (GPa)	3	4	5	6	8	10
$T_{\mathrm{N,sim}}$ (K)	600	607	615	620	633	643
$T_{\mathrm{N,exp}}$ (K)				590	600	610

Table 5: M. E. Gruner *et al.*

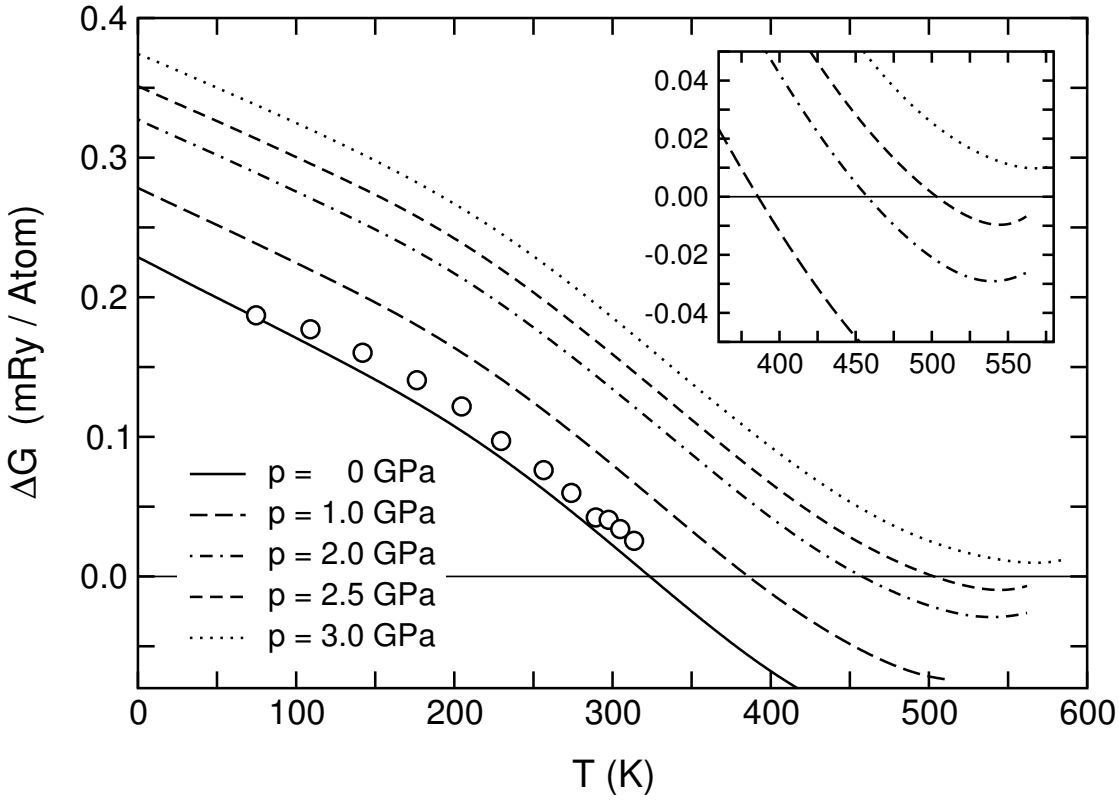

Figure 1: M. E. Gruner *et al.*

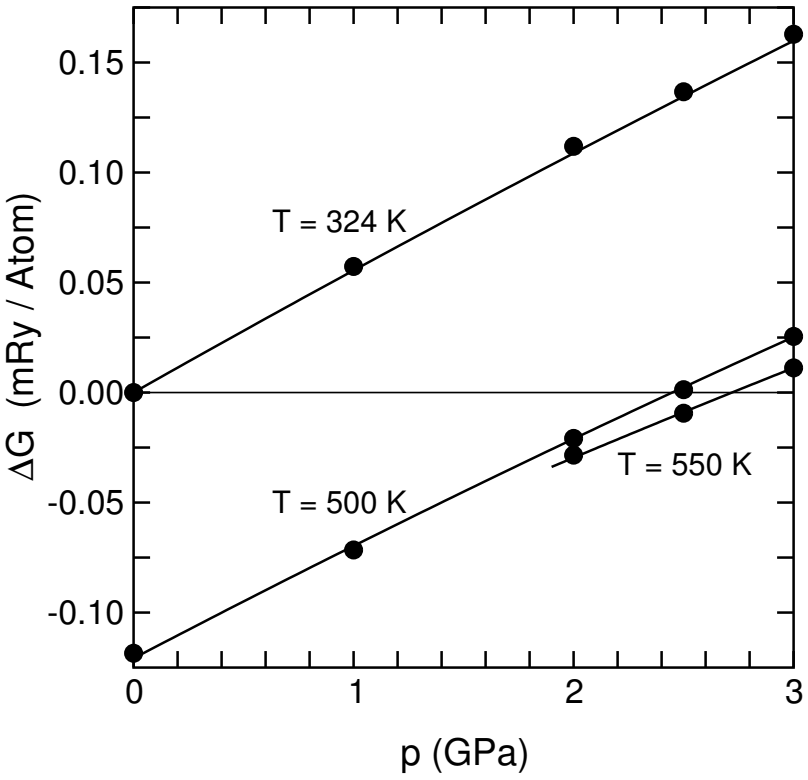

Figure 2: M. E. Gruner *et al.*

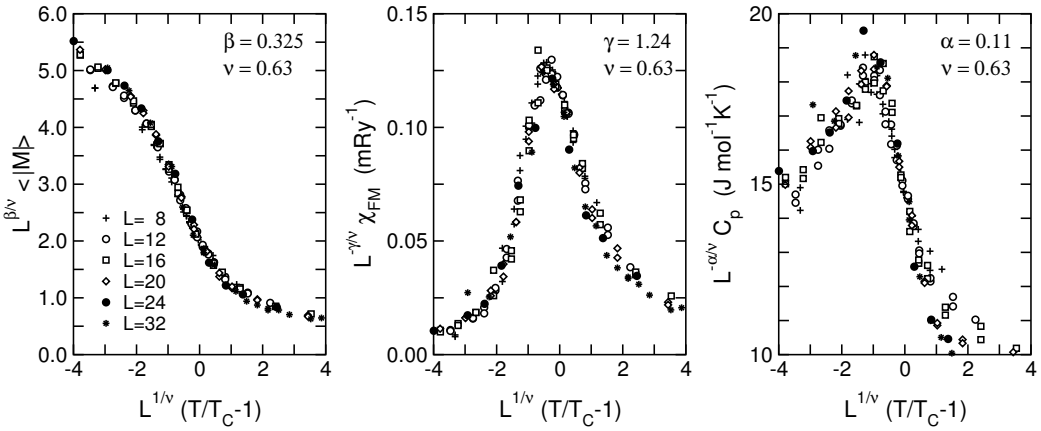

Figure 3: M. E. Gruner *et al.*

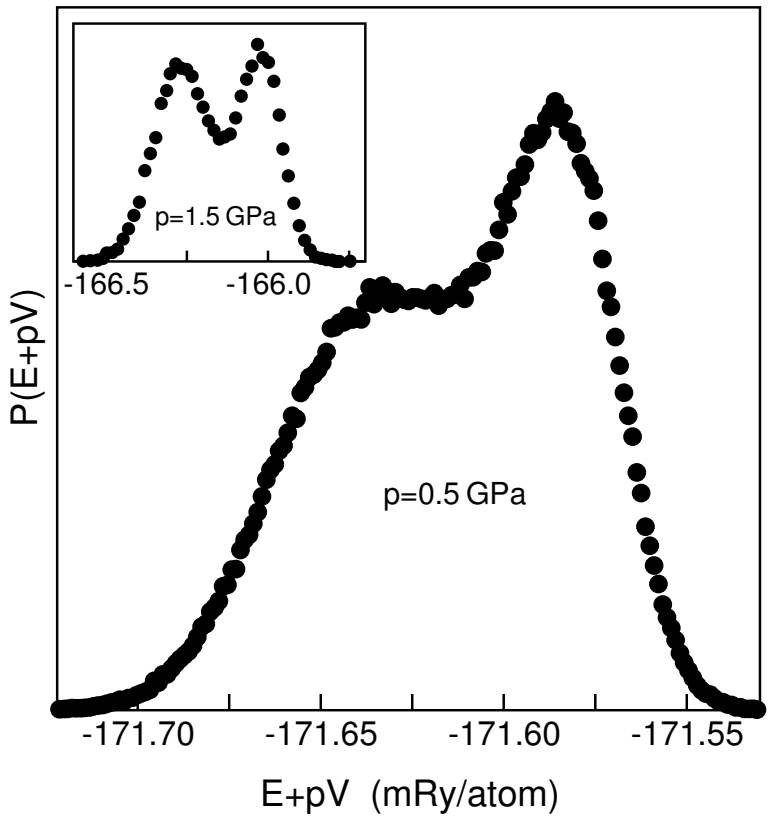

Figure 4: M. E. Gruner *et al.*

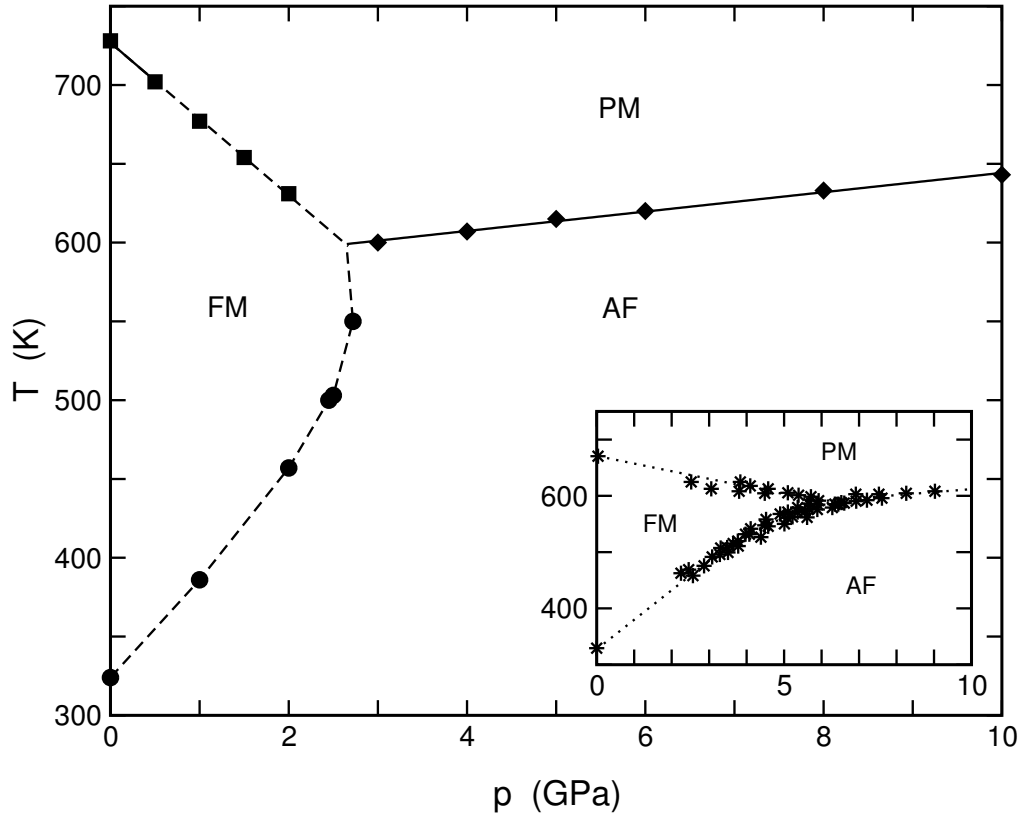

Figure 5: M. E. Gruner *et al.*